Regulation of microtubule dynamics by inhibition of the tubulin deacetylase HDAC6

Yuliya Zilberman[1], Christoph Ballestrem[2], Letizia Carramusa[1,3], Ralph Mazitschek[4], Saadi Khochbin[5] and Alexander Bershadsky[1,*]

[1]Department of Molecular Cell Biology, Weizmann Institute of Science, Rehovot 76100, Israel
[2]Wellcome Trust Centre for Cell-Matrix Research, Faculty of Life Sciences, University of Manchester, Manchester M13 9PT, UK
[3]Max Planck Institute for Metals Research, Department of New Materials and Biosystems, 70569 Stuttgart, Germany
[4]Broad Institute, Harvard University and Massachusetts Institute of Technology, Cambridge, MA 02141, USA
[5]INSERM, U823, Equipe epigénétique et signalisation cellulaire, Institut Albert Bonniot – Faculté de Médecine, Domaine de la Merci, 38706 La Tronche Cedex, France
*Author for correspondence (alexander.bershadsky@weizmann.ac.il)

Accepted 28 July 2009
Journal of Cell Science 122, 3531-3541 Published by The Company of Biologists 2009
doi:10.1242/jcs.046813

Summary

We studied the role of a class II histone deacetylase, HDAC6, known to function as a potent α-tubulin deacetylase, in the regulation of microtubule dynamics. Treatment of cells with the class I and II histone deacetylase inhibitor TSA, as well as the selective HDAC6 inhibitor tubacin, increased microtubule acetylation and significantly reduced velocities of microtubule growth and shrinkage. siRNA-mediated knockdown of HDAC6 also increased microtubule acetylation but, surprisingly, had no effect on microtubule growth velocity. At the same time, HDAC6 knockdown abolished the effect of tubacin on microtubule growth, demonstrating that tubacin influences microtubule dynamics via specific inhibition of HDAC6. Thus, the physical presence of HDAC6 with impaired catalytic activity, rather than tubulin acetylation per se, is the factor responsible for the alteration of microtubule growth velocity in HDAC6 inhibitor-treated cells. In support of this notion, HDAC6 mutants bearing inactivating point mutations in either of the two catalytic domains mimicked the effect of HDAC6 inhibitors on microtubule growth velocity. In addition, HDAC6 was found to be physically associated with the microtubule end-tracking protein EB1 and a dynactin core component, Arp1, both of which accumulate at the tips of growing microtubules. We hypothesize that inhibition of HDAC6 catalytic activity may affect microtubule dynamics by promoting the interaction of HDAC6 with tubulin and/or with other microtubule regulatory proteins.

Supplementary material available online at
http://jcs.biologists.org/cgi/content/full/122/19/3531/DC1

Key words: Arp1, EB1, TSA, Acetylation, Dynamic instability, Tubacin

Introduction

Control of microtubule assembly and disassembly determines the organization and function of microtubule arrays in living cells. The dynamic instability of individual microtubules enables the cell to rapidly reorganize the microtubule cytoskeleton in the course of cell polarization, migration and mitotic division (Gelfand and Bershadsky, 1991; Howard and Hyman, 2003; Joshi, 1998; Kirschner, 1987). This instability is based on the innate characteristics of microtubule subunits, αβ-tubulin heterodimers (Burbank and Mitchison, 2006; Mahadevan and Mitchison, 2005; Nogales and Wang, 2006); moreover, it is precisely regulated by a complex hierarchy of diverse microtubule-associated proteins, or MAPs. Some of these proteins bind along the microtubule lattice, whereas others affect microtubule dynamics by sequestering tubulin subunits; still others accumulate at the growing microtubule tips (Cassimeris, 1999; Desai and Mitchison, 1997; Heald and Nogales, 2002; Valiron et al., 2001). The versatile complexes formed by the plus-end-localized, evolutionary conserved 'end-tracking' proteins (e.g. EB1, APC, LIS1, CLIP170, CLASPs, the dynactin complex, and others) play a primary role in controlling the dynamic behavior of microtubules, and their ability to anchor to other cellular structures (Carvalho et al., 2003; Galjart and Perez, 2003; Lansbergen and Akhmanova, 2006; Morrison, 2007).

Potentially important mechanisms for controlling microtubule dynamics are the post-translational modifications of tubulin subunits. The αβ-tubulin heterodimer is subject to a variety of such modifications (Hammond et al., 2008; Verhey and Gaertig, 2007; Westermann and Weber, 2003). Removal of tyrosine (detyrosination) or Glu-Tyr dipeptide from the C-terminus of α-tubulin, polyglutamylation and polyglycylation of α- and β-tubulins, and phosphorylation of some tubulins, all occur at the acidic C-terminus of tubulin molecules located on the outer surface of the microtubule. Another ubiquitous microtubule modification, acetylation of α-tubulin, occurs on lysine 40 (Edde et al., 1991; L'Hernault and Rosenbaum, 1985; LeDizet and Piperno, 1987) which, according to structural data, is localized to the luminal face of the microtubule (Draberova et al., 2000; Nogales, 1999).

It is generally accepted that newly synthesized tubulin undergoes modifications when incorporated into microtubules, while reverse reactions occur mainly on depolymerized tubulin subunits (Westermann and Weber, 2003). Thus, post-translational tubulin modifications of various types accumulate in stable, long-lived microtubules, as observed in numerous studies (Hammond et al., 2008). Such a general correlation, however, masks the specific functions of particular modifications that have only recently begun to emerge. An interesting example is microtubule detyrosination (Thompson, 1982). For many years, this modification has been

used as a marker of microtubule stabilization (Bulinski and Gundersen, 1991), although its specific role in the regulation of microtubule dynamics remained unclear. However, it was recently found that the tyrosine residue at the C-terminus of α-tubulin is critically important for the recruitment of proteins bearing the so-called cytoskeleton-associated protein glycine-rich (CAP-Gly) domain to the microtubule plus-ends (Mishima et al., 2007; Peris et al., 2006); some of these proteins, such as CLIP-170 and $p150^{Glued}$, are known to be potent regulators of microtubule dynamics and targeting (Akhmanova and Hoogenraad, 2005). In addition, the affinity of the kinesin-1 motor as well as the depolymerizing motors MCAK and KIF2A for microtubules could also depend on microtubule tyrosination (Konishi and Setou, 2009; Liao and Gundersen, 1998; Peris et al., 2009). Thus, detyrosination is not just a marker of microtubule stability but indeed affects microtubule behavior, by modifying the affinity of microtubules to certain regulatory proteins.

The precise role of α-tubulin acetylation in the regulation of microtubule dynamics has still not been resolved. Similar to detyrosination, tubulin acetylation was also found to be a hallmark of stabilized microtubules (Piperno et al., 1987; Webster and Borisy, 1989). The acetylation does not significantly affect the polymerization or depolymerization of pure tubulin in vitro (Maruta et al., 1986). However, recent studies revealed that tubulin acetylation promotes kinesin-1 binding to microtubules (Dompierre et al., 2007; Reed et al., 2006). It was further shown that other microtubule modifications such as polyglutamylation (Ikegami et al., 2007) and detyrosination (Dunn et al., 2008) can affect the binding of certain motor proteins to microtubules.

Until recently, the enzyme(s) acetylating α-tubulin in mammalian cells had not been identified, but a novel study by Creppe et al. (Creppe et al., 2009) suggests that the acetyltransferase elongator complex can perform this function in neurons. The molecules that mediate the reverse reaction, deacetylation, were determined, and described in several studies. These include histone deacetylase 6 (HDAC6), a member of the class II histone deacetylases (Boyault et al., 2007a; Hubbert et al., 2002; Matsuyama et al., 2002; Zhang et al., 2003), and SIRT2, a class III NAD-dependent histone deacetylase (North et al., 2003). HDAC6 and SIRT2 form a cytoplasmic complex, and probably function in concert (Nahhas et al., 2007; North et al., 2003), though manipulation with HDAC6 alone is sufficient to significantly change the level of microtubule acetylation. HDAC6 overexpression leads to complete deacetylation of microtubules, whereas inhibition of HDAC6 by specific inhibitors, RNAi-mediated knockdown, or genetic knockout increased microtubule acetylation (Haggarty et al., 2003; Hubbert et al., 2002; Matsuyama et al., 2002; Zhang et al., 2008; Zhang et al., 2003).

Manipulations with HDAC6, however, produced contradictory results vis-à-vis its effect on microtubule dynamics. An early publication (Matsuyama et al., 2002), as well as a recent, more comprehensive study (Tran et al., 2007), indicate that the degree of microtubule acetylation correlates with resistance to some microtubule-disrupting drugs (Matsuyama et al., 2002), as well as with specific modifications in parameters characterizing microtubule dynamics (Tran et al., 2007). At the same time, several other studies claimed that increased microtubule acetylation had no effect on the dynamic behavior of microtubules (Haggarty et al., 2003; Palazzo et al., 2003; Zhang et al., 2008). In particular, cultured fibroblasts derived from HDAC6 knockout mice have apparently normal microtubule organization and stability, even though all microtubules in non-neural cells were hyperacetylated, as compared with the control (Zhang et al., 2008). In none of these studies, however, was a detailed analysis of the dynamic behavior of microtubules undertaken.

Thus, the possible function(s) of α-tubulin acetylation in the regulation of microtubule dynamics, as well as the role of modifying enzymes such as HDAC6, deserve careful elucidation. To this end, we investigated the effect of HDAC6 on microtubule dynamics in greater detail, using drugs that specifically inhibit HDAC6 deacetylase activity, RNAi to downregulate HDAC6 expression, and overexpression of wild-type or mutated HDAC6. Microtubule dynamics were studied directly, by means of time-lapse analysis of GFP-tubulin-labeled microtubules, and by measurement of microtubule growth using GFP- or RFP-labeled plus-end-tracking proteins such as EB1 and EB3. In addition, we utilized co-immunoprecipitation experiments to assess the association of HDAC6 with specific microtubule end-tracking proteins.

Using these approaches, we succeeded in demonstrating that HDAC6 is indeed involved in the control of microtubule dynamics. However, HDAC6-mediated microtubule regulation cannot be explained solely by alterations in the level of tubulin acetylation. Since the physical presence of HDAC6 appears to play a critical role in the acetylation-dependent regulation of microtubule dynamics, we propose that such regulation is controlled by a novel mechanism involving the interaction of HDAC6 with plus-end tip-binding proteins.

Results

Inhibition of HDAC6 deacetylase activity decreases the rates of microtubule growth and shrinkage

Previous studies indicated that HDAC6 activity can be inhibited by trichostatin A (TSA), a class I and II histone deacetylase inhibitor (Matsuyama et al., 2002), and by tubacin, a specific inhibitor of HDAC6 (Haggarty et al., 2003). We began by confirming that these inhibitors increase the level of α-tubulin acetylation in our experimental system, by treating B16F1 melanoma cells stably expressing GFP-tubulin (Ballestrem et al., 2000) with TSA or tubacin for 1 hour, and subsequently staining them for acetylated α-tubulin. In control, non-treated cells, only some microtubule segments in the central part of the cell were acetylated (Fig. 1Aa-c), whereas microtubules at the cell periphery usually lacked acetylated α-tubulin (Fig. 1Aa-c). At the same time, all microtubules in the tubacin-treated cells contained acetylated α-tubulin evenly distributed along their length (Fig. 1Ad-f). The effect of TSA was indistinguishable from that of tubacin (supplementary material Fig. S1). Western blots of cell lysates developed with antibody against acetylated α-tubulin revealed that treatment of the cells with either TSA or tubacin dramatically increased α-tubulin acetylation (Fig. 1B,C). TSA and tubacin efficiently increased the fraction of acetylated microtubules, as well as the amount of acetylated α-tubulin in CHO-K1 cells (data not shown).

We then tested whether inhibition of HDAC6 affects microtubule dynamics. In the first series of experiments, we used end-tracking EB1 protein fused to GFP for visualization of the growing microtubule plus-ends (Akhmanova and Hoogenraad, 2005; Mimori-Kiyosue et al., 2000). Visualization of EB1 together with total and acetylated tubulin revealed that endogenous EB1 forms ‘comet tails’ at the tips of both acetylated and non-acetylated microtubules (Fig. 2). Since overexpression of EB1 alone can affect microtubule dynamics (Ligon et al., 2003) (and our unpublished data), only cells expressing low levels of EB1 (in which EB1 was

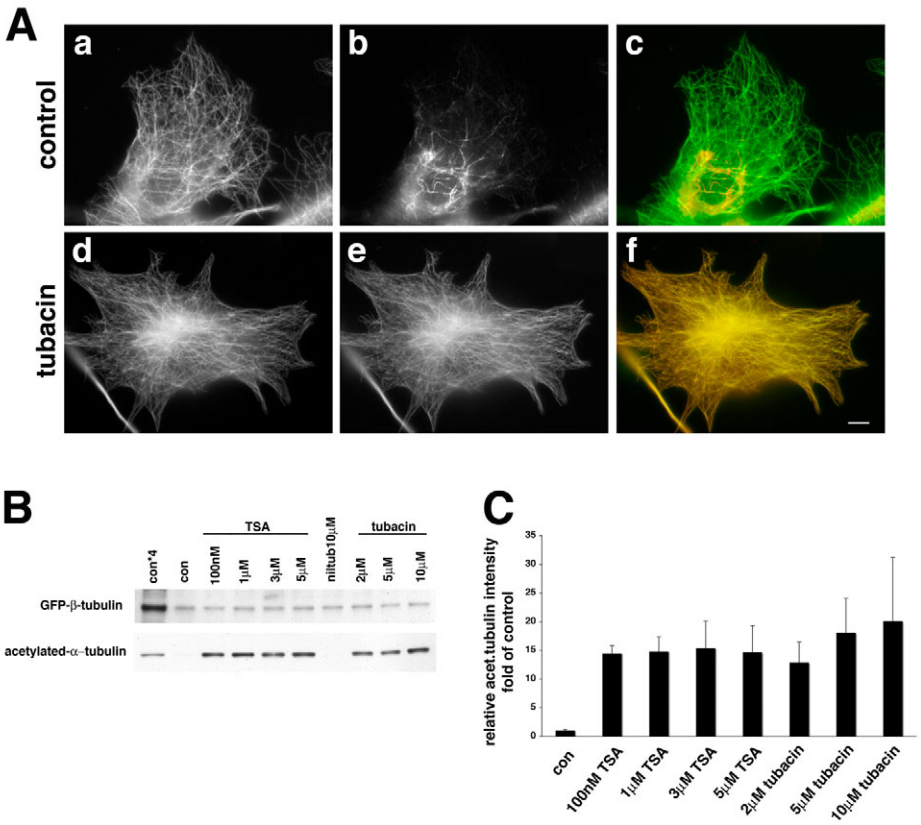

Fig. 1. (A) Effect of tubacin on microtubule acetylation. B16F1melanoma cells stably expressing GFP-tubulin (a,d) were stained for acetylated α-tubulin (b,e); merged images of control and tubacin-treated cells are shown in c and f, respectively. In merged images, GFP-tubulin was colored green, and acetylated tubulin red, so the acetylated microtubules look yellow. In control cells (a-c), acetylated α-tubulin was mostly incorporated into scattered microtubule segments (b), whereas in cells treated with 10 μM tubacin for 2 hours, essentially all microtubules contained acetylated α-tubulin (d-f). Scale bar: 8 μm. (B) Western blot of lysates of control cells, and cells treated for 2 hours with the indicated concentrations of TSA, niltubacin or tubacin. In the lane labeled con*4, the loaded total protein amount was 4 times higher than that loaded in the other lanes, in order to obtain a measurable value of acetylated tubulin in controls. In the sample treated with niltubacin, the intensity was similar to control (only visible at higher exposure). The upper panel shows the amount of β-tubulin-GFP in the samples of B16F1 cells labeled with anti-GFP antibody. The lower panel shows part of the same blot with shorter exposure time, in which the acetylated tubulin was stained. (C) Quantification of the western blot. For each sample, the ratio between the amounts of acetylated and total tubulin was calculated. The levels of tubulin acetylation are shown relative to the control value. Results are an average of three independent experiments, performed as in B. Note that there was a similar increase in acetylation level in all samples treated with varying doses of TSA or tubacin.

observed only as a 'comet tail' at the microtubule tips, but not along the entire microtubule length) were chosen to measure microtubule growth velocities. We further determined that, similar to endogenous EB1, the exogenous GFP-EB1 or RFP-EB1 localize equally well to the tips of acetylated and non-acetylated microtubules (supplementary material Fig. S2). In all, about two hundred comet tails were detected in both control and TSA-treated cells.

Growth velocity was then calculated by superimposing two successive images, and measuring the displacement of the microtubule tip. Careful inspection of the time-lapse movies showing the dynamics of such displacements (supplementary material Movie 1) revealed that microtubule growth velocity in control cells was essentially constant in the central part of the cell, but dropped significantly close to the cell edges. Thus, in our measurements of microtubule velocity using GFP-EB1 labeling, we concentrated on microtubule dynamics in the central part of the cell. Measurements taken at the cell edges were performed using GFP-tubulin labeling (see below).

Treatment of cells with deacetylase inhibitor significantly decreased the degree of tip displacement and, hence, instantaneous microtubule growth velocities (Fig. 3A; supplementary material Movies 2 and 3). In addition to tubacin and TSA, we employed two other treatments as controls: sodium butyrate, a broad-specificity deacetylase inhibitor that, however, does not affect HDAC6 activity (Guardiola and Yao, 2002); and niltubacin, an inactive analog of tubacin which also has no effect on HDAC6 deacetylase function (Haggarty et al., 2003), but interacts with the same and/or overlapping site(s) within the HDAC6 molecule (Cabrero et al., 2006). Fig. 3B shows that neither butyrate nor niltubacin affected the velocity of microtubule growth, but treatment with tubacin at a concentration of 10 μM reduced the velocity by 50%. TSA (5 μM) also significantly decreased microtubule growth velocity, as compared with butyrate (Fig. 3C).

Analysis of the distribution of microtubule growth velocities shown in Fig. 3D revealed that TSA reduces the growth velocities of all microtubules in the treated cells. Such distribution is inconsistent with a proposed model according to which a selected population of microtubules was hyperstabilized, whereas others were unaffected.

The same alteration in the distribution of growth velocities was observed in the tubacin-treated cells (data not shown). The effects of both tubacin and TSA on microtubule dynamics were dose-

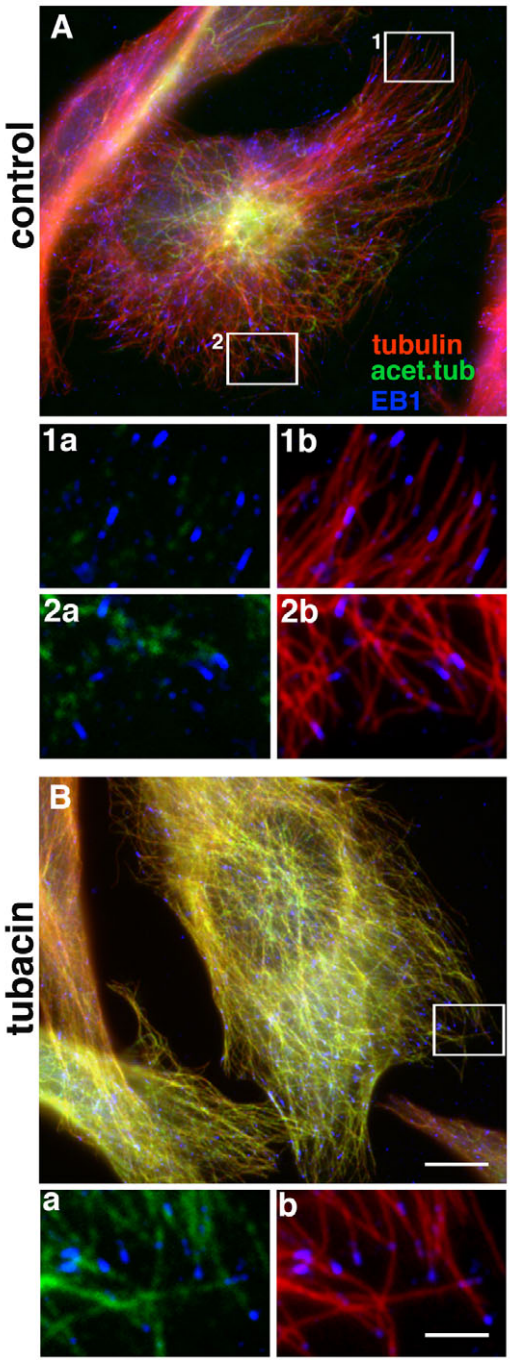

Fig. 2. Localization of the endogenous EB1 to the microtubules in control (A) and tubacin-treated (B) cells. B16F1 cell stably expressing GFP-tubulin (red) were stained with anti-EB1 (blue) and anti-acetylated tubulin (green) antibodies. The boxed regions are shown at higher magmification below A and B. (A1a, A2a, Ba) EB1 plus acetylated tubulin; (A1b, A2b, Bb) EB1 plus GFP-tubulin. Scale bars: 10 μm in A and B; 3.5 μm in 1a,b, 2a,b and a and b. EB1 comet tails are localized to the tips of both acetylated and non-acetylated microtubules. Note that on average, that the comet tails are shorter in tubacin-treated cells.

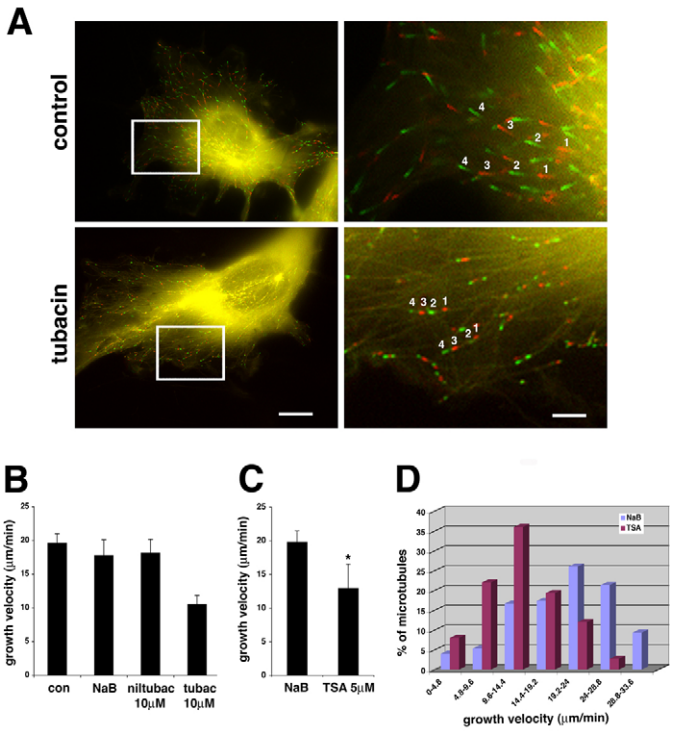

Fig. 3. Inhibition of HDAC6 activity decreases microtubule growth rate. (A) Measurements of microtubule growth velocities. Overlap of four successive time-lapse images of EB1-GFP taken at 5-second intervals. For purposes of presentation, the first and third images are colored red, and the second and fourth images are colored green. The boxed regions are shown at higher magnification on the right. Note that displacement of comet tails in control cell (upper row) is significantly greater than in cells treated with tubacin (lower row; see also Movies 2 and 3 in supplementary material). Scale bars: 10 μm (left panels); 2.5 μm (right panels). (B) Average instantaneous microtubule growth velocities in control cells, and in cells treated with NaB, niltubacin and tubacin. Only tubacin treatment decreased microtubule growth velocity, while NaB and niltubacin had no effect. Error bars represent standard errors of mean (s.e.m.). (C) Average growth velocity decreased by 40% in cells treated with 5 μM TSA, as compared to control cells treated with 10 mM NaB. Error bars show the s.e.m. *Significant difference between treatments [according to the Kolmogorov-Smirnov (KS) test, $P<0.001$]. Each bar in B and C represents the results from measurements of five cells, 30 microtubules per cell. (D) Distributions of microtubule growth velocities in control (blue bars) and TSA-treated (purple bars) B16F1cells. Approximately 750 measurements of microtubule velocity in 25 cells were taken for each data set.

dependent and reversible (supplementary material Fig. S3). The maximal effect on microtubule growth, about a 50% decrease, was reached at a concentration of 10 μM tubacin, and 3 μM of TSA (supplementary material Fig. S3). It is worth noting that 1 μM TSA did not produce any detectable effect on microtubule growth velocity (supplementary material Fig. S3B), while its effect on α-tubulin acetylation was already pronounced at 100 nM (Fig. 1B,C) in agreement with Dompierre et al. (Dompierre et al., 2007). The results of microtubule velocity measurements and effects of various inhibitors were similar in B16F1 and CHO-K1 cells (Fig. 3C; supplementary material Fig. S3; and data not shown).

As mentioned above, comparison of the growth velocity of GFP-EB1-decorated microtubules at the cell periphery versus those in the central part of the cell revealed a significant decrease in velocity at the lamellar edges of the cell (supplementary material Movie 1). In addition, close to the cell edge, microtubule ends alternate between phases of growth and shortening, a process known as dynamic instability (Cassimeris, 1999; Komarova et al., 2002; Sammak and Borisy, 1988; Shelden and Wadsworth, 1990). Since GFP-EB1 disappears from the microtubule ends when microtubules begin to shorten (Mimori-Kiyosue and Tsukita,

Table 1. Microtubule dynamic instability parameters in control (sodium butyrate-treated) and TSA-treated B16F1 cells

Parameter	NaB (10 mM)	TSA (5 μM)
Growth rate (μm/minute)	7.99±3.4	4.33±1.39*
Shortening rate (μm/minute)	14.18±7.17	6.35±2.7**
Catastrophe frequency (per second)	0.08±0.05	0.07±0.02
Rescue frequency (per second)	0.09±0.06	0.14±0.04
% Time in growing	37±13	37±11
% Time in pausing	33±10	45±13
% Time in shortening	28±15	18±6

Parameters of microtubule dynamic instability were measured at the cell periphery of living cells. Values are mean ± s.d. of 25 microtubules. The results of one of the three analogous experiments are presented. *P=0.0004, **P=0.0003, according to Student's t-test.

Table 2. Microtubule dynamic instability parameters in control (sodium butyrate-treated) and tubacin-treated B16F1 cells

Parameter	NaB (10 mM)	Tubacin (10 μM)
Growth rate (μm/minute)	5.85±1.53	3.96±1.03*
Shortening rate (μm/minute)	9.8±4.9	6.13±2.34**
Catastrophe frequency (per second)	0.07±0.04	0.08±0.03
Rescue frequency (per second)	0.12±0.05	0.12±0.04
% Time in growing	38±11	34±9
% Time in pausing	42±13	45±9
% Time in shortening	20±11	21±6

Parameters of microtubule dynamic instability were measured at the cell periphery of living cells. Values are mean ± s.d. of 21 microtubules. The results of one of the three analogous experiments are presented. *P=0.0001, **P=0.0034, according to the Student's t-test.

2003), it cannot be used for analysis of dynamic instability events. Fortunately, at the cell edge, unlike the central part of the cell, ends of individual microtubules labeled with GFP-tubulin can be resolved. Therefore, in the second series of experiments, we studied how inhibition of HDAC6 deacetylase affects the parameters characterizing the dynamic instability of microtubules, using B16F1 cells stably expressing tubulin-GFP (Ballestrem et al., 2000). Comparison of the growth velocities of microtubules labeled with GFP-EB1, with those labeled with GFP-tubulin at the cell periphery, yielded similar values, within a range of 5-10 μm/minute.

We found that inhibition of HDAC6 with TSA (Table 1) or tubacin (Table 2; supplementary material Fig. S4) reduced the growth velocities of microtubules labeled with tubulin-GFP. Shortening velocities of the microtubule ends located at the cell periphery were also reduced by about 50%, compared with those observed in control cells. Notably, other parameters characterizing microtubule dynamics, such as the frequency of 'catastrophe' (transitions from growth/pause to shortening) and 'rescue' (transitions from shortening to growth/pause) events, as well as the average amount of time spent by microtubules in the growing, pausing or shortening phases, did not change significantly when cells were treated with TSA or tubacin (Tables 1 and 2).

Knockdown of HDAC6 does not affect microtubule growth velocity

We further tested whether the reduction of HDAC6 levels by siRNA-driven gene silencing affects microtubule dynamics in the same manner as chemical inhibitors of HDAC6 deacetylase activity. As shown in Fig. 4A, cells transfected with HDAC6 siRNA expressed only trace levels of HDAC6 compared with cells transfected with control, 'scrambled' siRNA. To compare microtubule dynamics in control and HDAC6 knockdown cells, we co-transfected HDAC6 siRNA or scrambled siRNA duplexes with GFP-EB1, and determined microtubule acetylation and growth velocity as described above. In the cells transfected with scrambled siRNA, only a few perinuclear microtubules were acetylated (Fig. 4B, upper panel); however, knockdown of HDAC6, similarly to treatment with TSA or tubacin, led to complete acetylation of microtubules in the cell (Fig. 4B, middle and bottom panels).

Surprisingly, measurements of microtubule growth velocities did not reveal any difference between HDAC6 knockdown and control (scrambled siRNA-transfected) cells (Fig. 4C). At the same time, these cells differed in their sensitivity to tubacin: namely, tubacin treatment decreased microtubule growth velocity only in the HDAC6-containing cells transfected with scrambled siRNA, but not in the HDAC6 knockdown cells (Fig. 4C). These results indicate that tubacin affects microtubule dynamics via its specific effect on HDAC6, and that knockdown of HDAC6 alone does not affect microtubule growth. Moreover, total acetylation of microtubules in HDAC6 knockdown cells (treated or not treated with tubacin) was not sufficient to decrease microtubule growth velocity (Fig. 4B,C). Thus, the physical presence of HDAC6 in the cell, together with inhibition of its deacetylase activity, seems to be required to slow the rate of microtubule elongation.

HDAC6 mutants inhibit microtubule growth rate

Our aforementioned results suggest that it is not the acetylation of microtubules per se, but rather the presence of HDAC6 molecules with impaired enzymatic activity, that affect microtubule dynamics. Accordingly, we investigated whether expression of HDAC6 with mutations in its catalytic domains could affect microtubule dynamics. HDAC6 is a unique histone deacetylase in that it contains two deacetylase domains, both of which are required for normal deacetylase activity (Zhang et al., 2006). We therefore examined how expression of HDAC6-based constructs with impaired catalytic activity [described by Zhang et al. (Zhang et al., 2006)] affected microtubule dynamics. We compared the effects of the following constructs: wild-type HDAC6; HD1m, bearing inhibitory point mutations in the first catalytic domain; HD2m, bearing inhibitory point mutations in the second catalytic domain; and HD1/2m, in which both catalytic domains contained inhibitory mutations. Overexpression of wild-type HDAC6 reduced the level of acetylated α-tubulin in transfected cells, whereas the overexpression of any of the mutants did not produce such an effect (Fig. 5A). Our results showed that mutations in either of the two catalytic domains, HD1m or HD2m, produced a moderate, though significant, decrease in microtubule growth velocity, which was comparable with the decrease induced by deacetylase inhibitors (Fig. 5B). Overexpression of wild-type HDAC6, as well as the construct with mutations in both catalytic domains (HD1/2m), did not induce any changes in microtubule growth, as compared with control (Fig. 5B). Thus, an HDAC6 molecule with inhibitory mutations in one of the catalytic domains, but not in both, can slow microtubule growth.

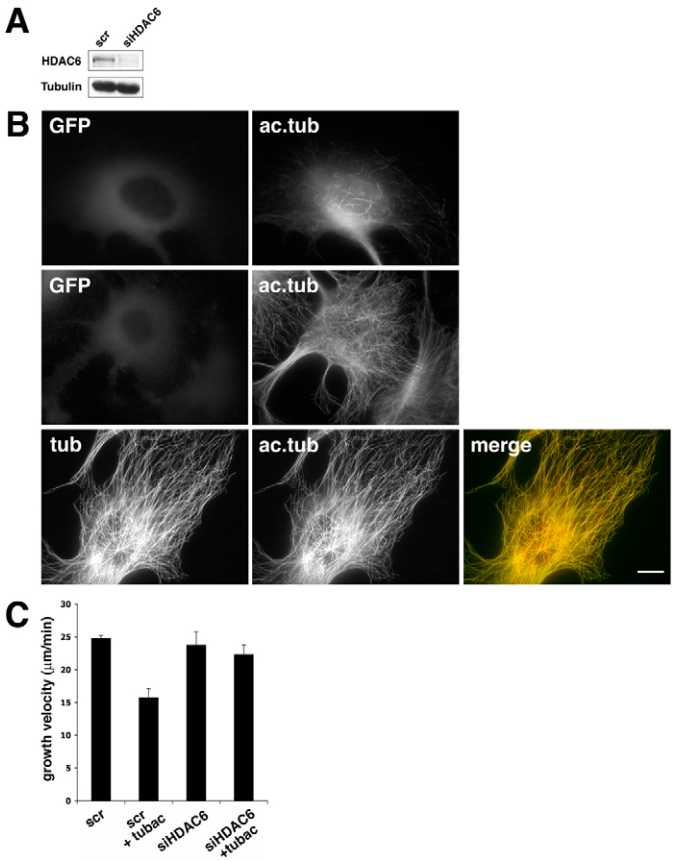

Fig. 4. Knockdown of HDAC6 increases microtubule acetylation, but does not affect the velocity of microtubule growth. (A) Western blot of cells transfected with a scrambled (scr) siRNA (control), and with siRNA specific for mouse HDAC6 (siHDAC6). Note the efficient knockdown of HDAC6 in cells treated with HDAC6 siRNA. Tubulin was probed as a loading control. (B) Control cells transfected with scrambled siRNA (upper panel) contain only a few segments of acetylated microtubules, whereas cells transfected with HDAC6-specific siRNA have a well-developed array of acetylated microtubules (middle panel). Transfected cells were labeled with GFP. Visualization of acetylated and total microtubules in cells containing HDAC6 siRNA revealed that all microtubules in such cells are acetylated (lower panel). Scale bar: 10 μm. (C) Growth rates of EB1-GFP-labeled microtubules in cells transfected with HDAC6-specific and scrambled siRNA. Tubacin (10 μM) decreased microtubule velocities in cells transfected with scrambled (control) siRNA. The knockdown of HDAC6 in cells transfected with siRNA specific for HDAC6 (siHDAC6) abolished the effect of the tubacin, but did not affect microtubule velocities in cells not treated with the drug. Each bar represents measurements of microtubule growth velocity in five cells, 30 microtubules in each.

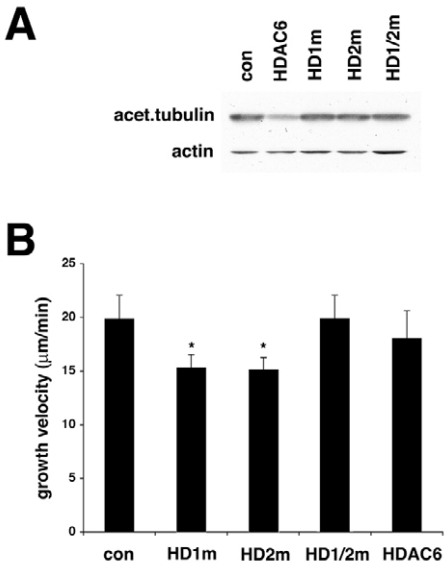

Fig. 5. HDAC6 mutants decrease the microtubule growth rate. (A) Western blot showing levels of tubulin acetylation in control cells, in cells overexpressing the wild-type HDAC6, and the three mutants with impaired deacetylating activity. HD1m and HD2m have inactivating mutations in the first and second deacetylase domains, respectively, of HDAC6. HD1/2m has mutations in both deacetylase domains of HDAC6. Note that overexpression of wild-type HDAC6 significantly decreases tubulin acetylation, whereas expression of all mutants has no effect on acetylation level. (B) Overexpression of mutants (HD1m and HD2m) triggered a minor, but significant, decrease in microtubule growth rate. The double mutant (HD1/2m), as well as wild-type HDAC6, does not affect the growth velocity of EB1-GFP-labeled microtubules. Error bars indicate the standard deviation of the velocities. Asterisks indicate a significant difference between the mutant and the control values (according to KS test, $P<0.001$). Each bar represents the measurements of microtubule growth velocity in five cells, 30 microtubules in each.

HDAC6 is associated with EB1 and Arp1, and affects their localization at microtubules

Since our results suggested that HDAC6 with impaired catalytic activity modulates microtubule dynamics, we next tested whether HDAC6 could interact with microtubule-associated proteins localized to microtubule tips. To this end, we coexpressed HA-tagged HDAC6 with GFP fusion constructs of EB1 and LIS1, known plus-end-tracking proteins, and Arp1, a marker of the dynactin complex. A co-immunoprecipitation experiment revealed the association of HDAC6 with EB1 and Arp1, but not with LIS1 (Fig. 6). We then analyzed the interaction between HDAC6 and EB1 in greater detail, using cells transfected simultaneously with GFP-EB1 and the constructs encoding various domains of HDAC6. We found that only the N- and C-termini of HDAC6, but not deacetylase domains 1 and 2, co-immunoprecipitate with EB1 (supplementary material Fig. S5). Since, according to published data, HDAC6 binds tubulin via its deacetylation domains (Zhang et al., 2003), the HDAC6 domains responsible for EB1 binding do not overlap with domains involved in tubulin binding.

Next, we examined how inhibition and downregulation of HDAC6 affects the localization of EB1 and Arp1 at the microtubule tips. At low expression levels, EB1-GFP- and Arp1-GFP-labeled microtubule plus-ends appeared as comet tails, as shown in Fig. 7A. In control cells, the morphology and average length of the comet tails were similar for both proteins (Fig. 7A, left column; Fig. 7B). Both knockdown of HDAC6 and inhibition of its deacetylase activity affected the appearance of Arp1 and EB1 comet tails, but in different ways. A typical line scan analysis of the distribution of fluorescence intensity along the microtubule end in control and TSA-treated cells is presented in Fig. 7B. Following HDAC6 inhibition with tubacin or TSA, the EB1 and Arp1 tails became significantly shorter (Fig. 2A1a, Fig. 2A2a, Fig. 2Ba, Fig. 7A,C; supplementary material Movies 2 and 3). Importantly, this decrease in comet tail length was detected both by staining of endogenous end-tracking proteins (Fig. 2) and by visualization of GFP-labeled proteins (Fig. 7; supplementary material Fig. S2). At the same time, HDAC6 knockdown did not affect the length of EB1-GFP tails, but resulted in longer Arp1-GFP-labeled tails (Fig. 7A,C). It is worth noting that changes in the lengths of EB1-GFP comet tails correlate with changes in the microtubule growth velocity induced by the corresponding treatments. Upon HDAC6 knockdown, however, the

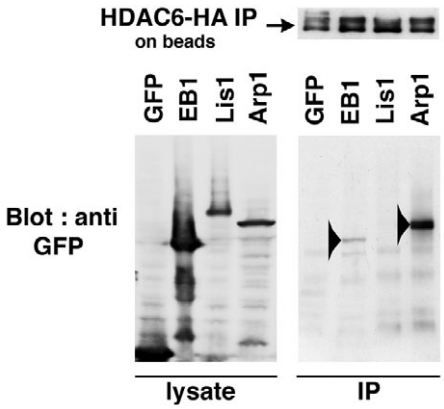

Fig. 6. HDAC6 interactions with microtubule end-tracking proteins. Upper panel: HDAC6-HA immunoprecipitated on the beads with anti-HA antibody. Left lower panel: GFP-labeled microtubule end-tracking proteins in the lysates of cells coexpressing these proteins with HA-tagged HDAC6. Right lower panel: GFP-labeled proteins co-immunoprecipitated with HDAC6 (see arrowheads). EB1 and Arp1, but not LIS1, co-immunoprecipitate with HDAC6.

Arp1-GFP comet tails lengthened, with no apparent change in microtubule growth velocity.

Discussion

The major aim of this study was to elucidate whether HDAC6 can affect microtubule dynamics, and, if so, to clarify the mechanism of its action. The results we obtained were surprising. Although the deacetylase inhibitors TSA and tubacin slowed microtubule growth, knockdown of HDAC6 did not produce any effect, although both HDAC6 inhibition and knockdown increased the acetylation of microtubules. Moreover, both tubacin and TSA affected microtubule growth at concentrations that are significantly higher than is necessary for maximal tubulin acetylation. These results do not indicate that the effects of the inhibitors were non-specific. On the contrary, our findings demonstrated that tubacin treatment (in high concentrations) did not produce any effect on microtubule growth velocity in the cells lacking HDAC6, thereby proving the specificity of this drug. In addition, niltubacin, which lacks the ability to inhibit HDAC6 deacetylase activity (Cabrero et al., 2006) did not affect microtubule growth velocity in our experiments. Thus, we conclude that a certain functional modification of HDAC6 triggered by its inhibition, rather than enhanced acetylation of tubulin per se, is responsible for the changes we observed in microtubule dynamics. This conclusion is supported by our finding that the expression of some HDAC6 mutants with impaired deacetylase activity can mimic the effects of tubacin or TSA on microtubule growth.

A closer look at the alterations in microtubule dynamics induced by HDAC6 inhibitors, provides clues for understanding the mechanism of such interactions. In the present study, we found that the effect of HDAC6 inhibitors on microtubule dynamics is unique: TSA and tubacin treatments inhibited the velocities of microtubule growth and shrinkage, but not the probabilities of transition from the growth to the shrinkage phase, and vice versa. This differs from the behavior of most known microtubule-associated proteins, which affect these probabilities, but not the growth and shrinkage rates themselves (Gelfand and Bershadsky, 1991; Heald and Nogales,

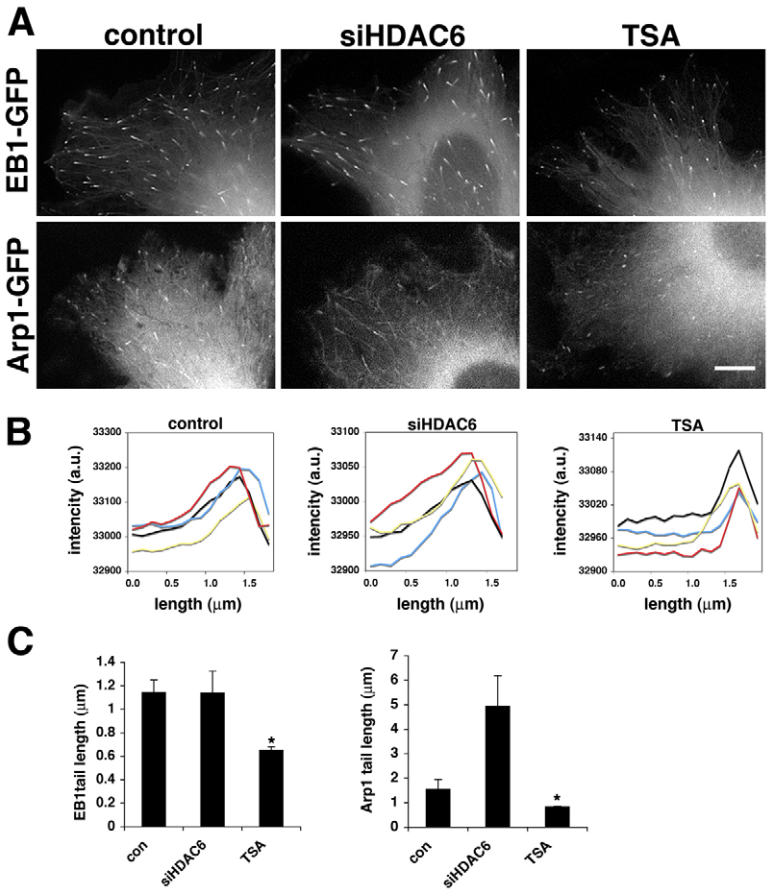

Fig. 7. (A) Localization of EB1-GFP and Arp1-GFP expressed in B16F1 cells. EB1 and Arp1 appear as comet tails in control cells (left column). HDAC6 knockdown did not affect EB1 localization, whereas the length of Arp1 comet tails significantly increased (middle column). In TSA-treated cells, the average length of the comet tails formed by both molecules decreased (right column). Scale bar: 5 μm. (B) Line-scan analysis of the intensity distribution in cells expressing EB1-GFP. Fluorescence intensity was measured along a 2 μm segment at the microtubule tip. Four typical microtubules for each cell type are shown in each panel. Note that the distribution of EB1 intensity in control and in HDAC6 knockdown cells is similar (left and center panels). At the same time, in TSA-treated cells, the peak of EB1 fluorescence intensity is narrower than that of controls (right panel). (C) Quantification of comet tail lengths of GFP-EB1 (left) and GFP-Arp1 (right) in control, HDAC6 knockdown and TSA-treated cells. *Significant difference between this value and the control value (according to KS test, $P<0.001$). Each bar represents the mean of 50 measurements.

2002; Howard and Hyman, 2003). Our observations, together with previous observations (Tran et al., 2007) are consistent with the idea that the inhibition of HDAC6 deacetylase activity leads to formation of a 'leaky cap' at the plus-end of microtubules, impeding both attachment and detachment of tubulin subunits. In fact, it is known from studies of actin dynamics that proteins forming leaky caps, such as formins, decrease the growth and shortening rates of actin filaments (Zigmond et al., 2003). In connection with this, it is interesting that HDAC6 forms complexes with microtubule end-tracking proteins EB1 and Arp1, which localize to the growing ends of microtubules. Moreover, inhibition of HDAC6 activity produces characteristic changes in the morphology and length of the comet tails formed by EB1-GFP and Arp1-GFP at the microtubule ends. Although the shortening of EB1 comet tails may arise from a corresponding decrease in microtubule growth velocity (Bieling et al., 2007), changes in Arp1 localization suggest that HDAC6 inhibition indeed produces some specific alterations at the microtubule tips.

Accordingly, we suggest a model that may account for the results described above, and provide some directions for future study. First, we propose that the HDAC6 molecule can function as a leaky cap at the microtubule end if its deacetylase function is impaired. This can occur via direct or indirect binding of HDAC6 to the microtubule end. The acetylated lysine 40 in α-tubulin is located at the luminal face of the microtubule wall (Draberova et al., 2000; Nogales et al., 1999), and therefore could be directly accessible from the microtubule end. Alternatively, HDAC6 could bind the tubulin dimer (containing acetylated α-tubulin) in the cytosol, and then attach to the microtubule's growing end in a complex with this dimer. This scenario resembles the well-known mechanism by which colchicine (and other microtubule drugs) bind to microtubule ends (Jordan and Wilson, 2004; Margolis and Wilson, 1977). Furthermore, association of HDAC6 with the end-tracking proteins EB1 and Arp1 may facilitate interaction of HDAC6 with the microtubule tip. We propose that at the moment when HDAC6 interacts with the growing end of the microtubule, it can form a plug, or cap, physically interfering with both the addition of new tubulin subunits, and the detachment of the tubulin subunits from the microtubule.

Under normal circumstances, HDAC6 quickly deacetylates α-tubulin and dissociates from the microtubule end, so that the capping activity should be very transient, and should not interfere with microtubule dynamics. However, impairment of deacetylase activity could lead to more prolonged contact between the HDAC6 molecule and the microtubule tip, making the capping activity of HDAC6 more pronounced. One possible mechanism could be based on the 'substrate trapping' activity of the inhibitor-treated or mutated HDAC6.

Substrate trapping mutants of some phosphatases, which show impaired phosphatase activity and are tightly associated with the phosphorylated substrates, were previously described (Blanchetot et al., 2005; Flint et al., 1997). We speculate that HDAC6 treated with tubacin or TSA, as well as HDAC6 mutants with mutations in one of their deacetylase domains (HD1m or HD2m) demonstrate such substrate trapping activity towards acetylated α-tubulin. The HDAC6 double mutant HD1/2m apparently does not have such activity, since its overexpression does not affect microtubule dynamics. It is worth noting that both tubacin and TSA interact with only one (C-terminal) deacetylase domain of HDAC6 (Haggarty et al., 2003), so the single-domain mutants should mimic the effects of the inhibitors better than the double-domain mutants. More detailed biochemical characterization of these mutants is required, in order to explain their varying effects on microtubule dynamics.

The proposed mechanism underlying the effect of HDAC6 inhibition on microtubule dynamics outlined above is still hypothetical, and other possible explanations should be considered. The list of HDAC6 'partners' with which it can interact either enzymatically or non-enzymatically, has expanded considerably during last several years. First, several other targets besides α-tubulin; namely, Hsp90 and cortactin (Kovacs et al., 2005; Zhang et al., 2007) were shown to be deacetylated by HDAC6. Cortactin is an actin-binding protein promoting Arp2/3-dependent actin nucleation (Ammer and Weed, 2008), whereas Hsp90 is also a potent regulator of actin polymerization, interacting with and enhancing the function of the N-WASP protein (Park et al., 2005). Involvement of Hsp90 in HDAC6-dependent actin remodeling was also recently reported (Gao et al., 2007). In addition, assembly of purified tubulin in vitro could be affected by Hsp90 (Garnier et al., 1998). Thus, cortactin and Hsp90, novel targets of HDAC6, could in principle mediate the effect of HDAC6 inhibition on microtubules acting, directly or indirectly, via remodeling of the actin cytoskeleton. The putative participation of Hsp90 or cortactin in the effect of HDAC6 inhibition on microtubule dynamics requires the physical presence of HDAC6, rather than just increased acetylation of Hsp90 or cortactin, since HDAC6 knockdown, which enhances such acetylation, is not sufficient for alteration of microtubule dynamics.

In addition to novel HDAC6 deacetylation targets, a broad group of proteins that can interact with HDAC6 non-enzymatically was recently discovered. Among this group of diverse proteins are estrogen receptor alpha, which may form a complex with HDAC6 and tubulin at the plasma membrane (Azuma et al., 2009); farnesyltransferase, which forms a complex with HDAC6 on microtubules (Zhou et al., 2009); BBIP10, which participates in trafficking inside the primary cilium (Loktev et al., 2008); and parkin, which accumulates in the centrosome in a microtubule-dependent manner, forming a complex with HDAC6 (Jiang et al., 2008). In nerve cells, HDAC6 interacts with the microtubule-associated protein tau (Ding et al., 2008), which inhibits its deacetylase function (Perez et al., 2009). It was previously shown that HDAC6 forms a complex with the phosphatase PP1 (Brush et al., 2004) and interacts with cytoplasmic dynein (Kawaguchi et al., 2003). Finally, HDAC6 may interact with formin homology proteins mDia2 and mDia1 (Bershadsky et al., 2006; Destaing et al., 2005).

Among the partners of HDAC6 listed above, there are obvious candidates that could participate in HDAC6-dependent microtubule regulation. In particular, inhibited HDAC6 could form tighter or weaker complexes with these proteins, which could affect their microtubule regulatory functions. Such regulation can occur on microtubules, or could operate via sequestration and removal of regulatory proteins by inhibited HDAC6. Thus, in addition to the mechanism outlined above involving EB1 and Arp1, several other pathways involving different partners of HDAC6 may be proposed. Clarification of the exact mechanism awaits future studies.

Irrespective of the particular mechanism involved, our study demonstrates that HDAC6 knockdown does not affect microtubule dynamics, although HDAC6 with impaired enzymatic activity produces specific alterations in microtubule growth. These results are consistent with a recent study showing that development of HDAC6 knockout mice proceeds normally, despite increased tubulin acetylation in all non-neuronal tissues (Zhang et al., 2008).

It is also worth noting that another effect of HDAC6 inhibition, namely, destabilization of ERBB2 mRNA, also requires the physical presence of HDAC6, and cannot be reproduced by HDAC6 knockdown (Scott et al., 2008). HDAC6 has been shown to be a key regulator of the cellular response to stress, participating, in particular, in aggresome formation (Boyault et al., 2007b; Kawaguchi et al., 2003; Kwon et al., 2007; Matthias et al., 2008). Since aggresome formation depends on microtubule-mediated processes, the physiological modulation of HDAC6 deacetylase activity may play a role in the process of microtubule regulation under these conditions. Another system in which HDAC6 may play a role as a physiological regulator of microtubule dynamics is the process of immunological synapse formation (Serrador et al., 2004; Valenzuela-Fernandez et al., 2008). Finally, since inhibitors of class II deacetylases are regarded as potential anti-cancer drugs, it is necessary to take into consideration the fact that they are capable of affecting microtubule dynamics, by inhibition of HDAC6.

Materials and Methods

Chemicals and cell cultures

Sodium butyrate, trichostatin A (TSA) and fibronectin were purchased from Sigma (Sigma, St Louis, MO). Tubacin and niltubacin were characterized previously (Haggarty et al., 2003).

Chinese hamster ovary cells (CHOK1) cells were obtained from American Type Tissue Culture (ATCC, Rockville, MD) and cultured in F12 nutrient mixture (Gibco, Rhenium, Jerusalem, Israel) supplemented with 10% bovine calf serum (Hyclone, Logan, UT), 1% L-glutamine (Biological Industries, Kibbutz Beit Haemek, Israel) and 1% penicillin-streptomycin solution (Sigma). HEK293T cells were cultured in Dulbecco's modified Eagle's medium (DMEM; Gibco), containing the same supplements. B16F1 melanoma cells stably transfected with β-tubulin-GFP (Ballestrem et al., 2000) were cultured in DMEM with 10% FCS, 2 mM glutamine, and antibiotics. Trypsin-EDTA (Biological Industries) was used to subculture the cells. Phosphate-buffered saline (PBS; Gibco) was used to wash the cells. Transfections for immunostaining were performed in 36 mm dishes with Lipofectamine Plus (Rhenium, Jerusalem, Israel), according to the manufacturer's instructions. Transfection of HEK293T cells for co-immunoprecipitation was performed on 100 mm dishes, using the calcium phosphate method. Six hours after transfection, cells were washed with warm DMEM and left for 20 hours in the growth medium, prior to lysate preparation.

Plasmids

Plasmids used in our experiments [mHDAC6-HA, HDAC6-HA (HD1/2m), HDAC6-HA (HD1m), HDAC6-HA (HD2m)] were previously described (Zhang et al., 2006). The HDAC6 mutants had the following structures: HD1m, in which Asp250 and Asp252 were replaced by Asn; His254 and His255 were replaced by Val; HD2m, in which Asp648 was replaced by Asn, and His650 and His651 were replaced by Val (Zhang et al., 2006). The HDAC6 domain constructs HA-N-terminus, HA-DD1, HA-DD2, and HA-C-terminus were previously described (Zhang et al., 2003). EB1-GFP was obtained from Shoichiro Tsukita's laboratory, Department of Cell Biology, Kyoto University Faculty of Medicine, Kyoto, Japan (Mimori-Kiyosue et al., 2000). LIS1-GFP was kindly provided by Orly Reiner (Weizmann Institute of Science, Rehovot, Israel). Arp1-encoding plasmid was kindly provided by Erika Holzbaur (University of Pennsylvania, Philadelphia, PA). GFP was linked to Arp1 with the forward and reverse primers 5′-ATGGTACCATGGTGAGCAAGGGC-3′ and 3′-ATGGTAC-CCCCAGACCCCTTGTACAGCTCGTCCATG-5′, respectively. GFP was inserted into the plasmid using the *Kpn*I cloning site.

siRNA knockdown of HDAC6

siRNA specific for the HDAC6 mRNA sequence, and the 'scrambled' siRNA control sequence, were purchased from Santa Cruz Biotechnology (Santa Cruz, CA). Co-transfection of HDAC6 siRNA or scrambled siRNA with the indicated plasmids into B16 cells was performed with Lipofectamine 2000 in six-well plates, according to the manufacturer's protocol. Transfection with both HDAC6-specific and scrambled siRNA was repeated after 24 hours and 48 hours. Following the last transfection, cells were incubated for 3 hours, and then plated at a lower density onto 35 mm fibronectin-coated dishes (20 μg/ml in PBS for 1 hour at room temperature) and kept in culture for an additional 24 hours. The level of HDAC6 was determined by western blotting, using anti-HDAC6 rabbit polyclonal antibody (Santa Cruz Biotechnology). The microtubule growth velocity was assessed 72 hours after the first transfection.

Immunoprecipitation

HEK293T cells were used for immunoprecipitation experiments. Cells were washed twice with PBS and lysed 24 hours after transfection in 500 μl cold IP buffer [120 mM NaCl, 50 mM Tris pH 7.5, 10 mM $MgCl_2$, 2.5 mM EGTA, 1% Triton X-100, and a complete protease inhibitor cocktail tablet (the latter obtained from Roche)] for 15 minutes on ice. Lysates were centrifuged (13,000 ***g***, 15 minutes at 4°C), and the supernatant was then pre-cleared with 20 μl of protein A/G PLUS-agarose beads (Santa Cruz Biotechnology) for 1 hour at 4°C with gentle agitation. After transferring lysates to new tubes, primary antibody was added. The mixture was then incubated for 1 hour at 4°C with gentle agitation, and for an additional 1 hour with 30 μl of protein A/G PLUS-agarose beads. Beads were washed three times in immunoprecipitation (IP) buffer, and proteins were eluted in 40 μl of sample buffer, boiled for 5 minutes, and loaded onto an SDS-PAGE gel.

In the HDAC6 co-immunoprecipitation studies with microtubule end-tracking proteins, HDAC6-HA was expressed together with GFP-tagged EB1, LIS1 and Arp1. Anti-HA rat monoclonal antibody was used for precipitation (1:100, clone 3F10; Roche), and western blots were probed with a mouse monoclonal anti-GFP antibody (1:1000, Roche).

Immunostaining and fluorescence microscopy

Following transfection, cells were plated on glass coverslips coated with fibronectin (20 μg/ml). Cells were then cultured for 24 hours, prior to treatment with drugs and fixation.

For microtubule staining, cells were fixed and simultaneously permeabilized at 37°C in a mixture of 3% paraformaldehyde in PBS, 0.25% Triton X-100 (Sigma), and 0.2% glutaraldehyde for 15 minutes, and then washed twice in PBS for 10 minutes each time. Before staining, cells were treated with sodium borohydride in cytoskeleton buffer (CB; containing 10 mM MES, 150 mM NaCl, 5 mM EGTA, 5 mM $MgCl_2$ and 5 mM glucose, pH 6.1) for 15 minutes on ice.

For EB1 staining, cells were fixed in a 1 mM concentration of EGTA in 100% methanol for 10 minutes at –20°C, followed by 15 minutes fixation in 3% paraformaldehyde in phosphate-buffered saline (PBS). Cells were then treated for 5 minutes in 0.15% Triton-X-100 in PBS, blocked for 10 minutes in 1% bovine serum albumin (BSA), and labeled with antibodies.

Mouse anti-acetylated tubulin antibodies (1:500, 6-11B-1, Sigma) were used for staining of acetylated tubulin. Total tubulin was stained with anti-α-tubulin antibodies (1:500, DM1A; Sigma) and anti-EB1 goat antibody (1:50; Santa Cruz Biotechnology). The same primary antibodies were used for western blots. Secondary antibodies employed were: Cy3 donkey anti-goat (1:200, Jackson Laboratories), Cy3 goat anti-mouse (1:200, Jackson Laboratories) or Cy5 goat anti-mouse (1:80, Jackson Laboratories).

Fluorescence images were captured with an Olympus IX71 inverted fluorescence microscope equipped with a CCD camera (Cool SNAP HQ, Photometrics, Tucson, AZ), and controlled by a Delta Vision system (Applied Precision, Issaquah, WA). Images were saved as TIFF files using PRISM software (API, USA) on a Silicon Graphics computer, and arranged into figures using Adobe Photoshop.

Video microscopy

Images were recorded on an Olympus IX71 inverted fluorescence microscope using an Olympus 100× 1.3 NA UplanFI objective. The system was equipped with a Box & Temperature control system (Life Imaging Services, Basel, Switzerland; www.lis.ch/) and a CCD camera (Cool SNAP HQ, Photometrics) and was controlled by a Delta Vision system (Applied Precision). A dichroic mirror, and excitation and emission filter wheels (Chroma Technology, Rockingham, VT) were adjusted for detection of FITC, DAPI, Rhodamine and Cy5.

For EB1-GFP recordings, CHO-K1 or B16F1 cells were transfected with the plasmids indicated above, and then plated on fibronectin-coated glass-bottom dishes (MatTek Corporation, Ashland, MA). Following transfection (24-36 hours later), cells were plated in 25 mM Hepes-buffered complete DMEM medium, and placed under the microscope. Only cells with low levels of EB1-GFP expression were chosen for recordings. In other experiments, we used B16F1 cells stably transfected with β-tubulin-GFP (Ballestrem et al., 2000). Time-lapse recordings of transfected cells were performed at 5-second intervals. For measurements of microtubule dynamics in drug-treated cells, cells were plated as described above, and incubated with drugs at 37°C for 1 hour, before the start of recording.

Image analysis

For measurements of microtubule dynamics, two successive images from time-lapse recordings of cells expressing tubulin-GFP or EB1-GFP, taken at 5-second intervals, were colored red and green, respectively, using Openlab software (Improvision, www.improvision.com/). Images were then merged, so that the relative displacement of microtubule tips during the specified time period could be visualized. Measurements of microtubule growth velocity using GFP-EB1 were performed in five cells, 30 microtubules per cell, for each type of experimental condition.

Growth and shrinkage rates of microtubules labeled with GFP-tubulin were determined using the measurement tools of the Openlab software. Data were then transferred to Microsoft Excel files to calculate the indicated dynamic instability parameters. Parameters were calculated as previously described (Wittmann et al.,

2004). Only microtubule length changes exceeding the optical resolution of 0.2 μm per frame were considered as growth or shortening events. Transitions from growth to shortening, and from pauses to shortening (only if the pause was preceded by growth) were considered as catastrophe events; transition from shortening to growth and shortening to pauses (only if shortening preceded the pause) were considered as rescue events. Catastrophe (or rescue) frequencies were calculated as the number of events divided by the time of growth (or shortening). To determine each value, a minimum of five cells was analyzed. In each cell, five to ten microtubules were analyzed, with around 30 measurements per single microtubule. Each type of measurement was performed on two or three independent cultures.

The authors are grateful to Barbara Morgenstern for editorial assistance. A.B. holds the Joseph Moss Professorial Chair in Biomedical Research. His work was partially supported by the Israel Science Foundation, the Minerva Foundation, and the Maurice Janin Fund.

References

Akhmanova, A. and Hoogenraad, C. C. (2005). Microtubule plus-end-tracking proteins: mechanisms and functions. *Curr. Opin. Cell Biol.* **17**, 47-54.

Ammer, A. G. and Weed, S. A. (2008). Cortactin branches out: roles in regulating protrusive actin dynamics. *Cell Motil. Cytoskeleton* **65**, 687-707.

Azuma, K., Urano, T., Horie-Inoue, K., Hayashi, S., Sakai, R., Ouchi, Y. and Inoue, S. (2009). Association of estrogen receptor alpha and histone deacetylase 6 causes rapid deacetylation of tubulin in breast cancer cells. *Cancer Res.* **69**, 2935-2940.

Ballestrem, C., Wehrle-Haller, B., Hinz, B. and Imhof, B. A. (2000). Actin-dependent lamellipodia formation and microtubule-dependent tail retraction control-directed cell migration. *Mol. Biol. Cell* **11**, 2999-3012.

Bershadsky, A. D., Ballestrem, C., Carramusa, L., Zilberman, Y., Gilquin, B., Khochbin, S., Alexandrova, A. Y., Verkhovsky, A. B., Shemesh, T. and Kozlov, M. M. (2006). Assembly and mechanosensory function of focal adhesions: experiments and models. *Eur. J. Cell Biol.* **85**, 165-173.

Bieling, P., Laan, L., Schek, H., Munteanu, E. L., Sandblad, L., Dogterom, M., Brunner, D. and Surrey, T. (2007). Reconstitution of a microtubule plus-end tracking system in vitro. *Nature* **450**, 1100-1105.

Blanchetot, C., Chagnon, M., Dube, N., Halle, M. and Tremblay, M. L. (2005). Substrate-trapping techniques in the identification of cellular PTP targets. *Methods* **35**, 44-53.

Boyault, C., Sadoul, K., Pabion, M. and Khochbin, S. (2007a). HDAC6, at the crossroads between cytoskeleton and cell signaling by acetylation and ubiquitination. *Oncogene* **26**, 5468-5476.

Boyault, C., Zhang, Y., Fritah, S., Caron, C., Gilquin, B., Kwon, S. H., Garrido, C., Yao, T. P., Vourc'h, C., Matthias, P. et al. (2007b). HDAC6 controls major cell response pathways to cytotoxic accumulation of protein aggregates. *Genes Dev.* **21**, 2172-2181.

Brush, M. H., Guardiola, A., Connor, J. H., Yao, T. P. and Shenolikar, S. (2004). Deactylase inhibitors disrupt cellular complexes containing protein phosphatases and deacetylases. *J. Biol. Chem.* **279**, 7685-7691.

Bulinski, J. C. and Gundersen, G. G. (1991). Stabilization of post-translational modification of microtubules during cellular morphogenesis. *BioEssays* **13**, 285-293.

Burbank, K. S. and Mitchison, T. J. (2006). Microtubule dynamic instability. *Curr. Biol.* **16**, R516-R517.

Cabrero, J. R., Serrador, J. M., Barreiro, O., Mittelbrunn, M., Naranjo-Suarez, S., Martin-Cofreces, N., Vicente-Manzanares, M., Mazitschek, R., Bradner, J. E., Avila, J. et al. (2006). Lymphocyte chemotaxis is regulated by histone deacetylase 6, independently of its deacetylase activity. *Mol. Biol. Cell* **17**, 3435-3445.

Carvalho, P., Tirnauer, J. S. and Pellman, D. (2003). Surfing on microtubule ends. *Trends Cell Biol.* **13**, 229-237.

Cassimeris, L. (1999). Accessory protein regulation of microtubule dynamics throughout the cell cycle. *Curr. Opin. Cell Biol.* **11**, 134-141.

Creppe, C., Malinouskaya, L., Volvert, M. L., Gillard, M., Close, P., Malaise, O., Laguesse, S., Cornez, I., Rahmouni, S., Ormenese, S. et al. (2009). Elongator controls the migration and differentiation of cortical neurons through acetylation of alpha-tubulin. *Cell* **136**, 551-564.

Desai, A. and Mitchison, T. J. (1997). Microtubule polymerization dynamics. *Annu. Rev. Cell Dev. Biol.* **13**, 83-117.

Destaing, O., Saltel, F., Gilquin, B., Chabadel, A., Khochbin, S., Ory, S. and Jurdic, P. (2005). A novel Rho-mDia2-HDAC6 pathway controls podosome patterning through microtubule acetylation in osteoclasts. *J. Cell Sci.* **118**, 2901-2911.

Ding, H., Dolan, P. J. and Johnson, G. V. (2008). Histone deacetylase 6 interacts with the microtubule-associated protein tau. *J. Neurochem.* **106**, 2119-2130.

Dompierre, J. P., Godin, J. D., Charrin, B. C., Cordelieres, F. P., King, S. J., Humbert, S. and Saudou, F. (2007). Histone deacetylase 6 inhibition compensates for the transport deficit in Huntington's disease by increasing tubulin acetylation. *J. Neurosci.* **27**, 3571-3583.

Draberova, E., Viklicky, V. and Draber, P. (2000). Exposure of lumenal microtubule sites after mild fixation. *Eur. J. Cell Biol.* **79**, 982-985.

Dunn, S., Morrison, E. E., Liverpool, T. B., Molina-Paris, C., Cross, R. A., Alonso, M. C. and Peckham, M. (2008). Differential trafficking of Kif5c on tyrosinated and detyrosinated microtubules in live cells. *J. Cell Sci.* **121**, 1085-1095.

Edde, B., Rossier, J., Le Caer, J. P., Berwald-Netter, Y., Koulakoff, A., Gros, F. and Denoulet, P. (1991). A combination of posttranslational modifications is responsible for the production of neuronal alpha-tubulin heterogeneity. *J. Cell Biochem.* **46**, 134-142.

Flint, A. J., Tiganis, T., Barford, D. and Tonks, N. K. (1997). Development of "substrate-trapping" mutants to identify physiological substrates of protein tyrosine phosphatases. *Proc. Natl. Acad. Sci. USA* **94**, 1680-1685.

Galjart, N. and Perez, F. (2003). A plus-end raft to control microtubule dynamics and function. *Curr. Opin. Cell Biol.* **15**, 48-53.

Gao, Y. S., Hubbert, C. C., Lu, J., Lee, Y. S., Lee, J. Y. and Yao, T. P. (2007). Histone deacetylase 6 regulates growth factor-induced actin remodeling and endocytosis. *Mol. Cell. Biol.* **27**, 8637-8647.

Garnier, C., Barbier, P., Gilli, R., Lopez, C., Peyrot, V. and Briand, C. (1998). Heat-shock protein 90 (hsp90) binds in vitro to tubulin dimer and inhibits microtubule formation. *Biochem. Biophys. Res. Commun.* **250**, 414-419.

Gelfand, V. I. and Bershadsky, A. D. (1991). Microtubule dynamics: mechanism, regulation, and function. *Annu. Rev. Cell Biol.* **7**, 93-116.

Guardiola, A. R. and Yao, T. P. (2002). Molecular cloning and characterization of a novel histone deacetylase HDAC10. *J. Biol. Chem.* **277**, 3350-3356.

Haggarty, S. J., Koeller, K. M., Wong, J. C., Grozinger, C. M. and Schreiber, S. L. (2003). Domain-selective small-molecule inhibitor of histone deacetylase 6 (HDAC6)-mediated tubulin deacetylation. *Proc. Natl. Acad. Sci. USA* **100**, 4389-4394.

Hammond, J. W., Cai, D. and Verhey, K. J. (2008). Tubulin modifications and their cellular functions. *Curr. Opin. Cell Biol.* **20**, 71-76.

Heald, R. and Nogales, E. (2002). Microtubule dynamics. *J. Cell Sci.* **115**, 3-4.

Howard, J. and Hyman, A. A. (2003). Dynamics and mechanics of the microtubule plus end. *Nature* **422**, 753-758.

Hubbert, C., Guardiola, A., Shao, R., Kawaguchi, Y., Ito, A., Nixon, A., Yoshida, M., Wang, X. F. and Yao, T. P. (2002). HDAC6 is a microtubule-associated deacetylase. *Nature* **417**, 455-458.

Ikegami, K., Heier, R. L., Taruishi, M., Takagi, H., Mukai, M., Shimma, S., Taira, S., Hatanaka, K., Morone, N., Yao, I. et al. (2007). Loss of alpha-tubulin polyglutamylation in ROSA22 mice is associated with abnormal targeting of KIF1A and modulated synaptic function. *Proc. Natl. Acad. Sci. USA* **104**, 3213-3218.

Jiang, Q., Ren, Y. and Feng, J. (2008). Direct binding with histone deacetylase 6 mediates the reversible recruitment of parkin to the centrosome. *J. Neurosci.* **28**, 12993-13002.

Jordan, M. A. and Wilson, L. (2004). Microtubules as a target for anticancer drugs. *Nat. Rev. Cancer* **4**, 253-265.

Joshi, H. C. (1998). Microtubule dynamics in living cells. *Curr. Opin. Cell Biol.* **10**, 35-44.

Kawaguchi, Y., Kovacs, J. J., McLaurin, A., Vance, J. M., Ito, A. and Yao, T. P. (2003). The deacetylase HDAC6 regulates aggresome formation and cell viability in response to misfolded protein stress. *Cell* **115**, 727-738.

Kirschner, M. W. (1987). Biological implications of microtubule dynamics. *Harvey Lect.* **83**, 1-20.

Komarova, Y. A., Akhmanova, A. S., Kojima, S., Galjart, N. and Borisy, G. G. (2002). Cytoplasmic linker proteins promote microtubule rescue in vivo. *J. Cell Biol.* **159**, 589-599.

Konishi, Y. and Setou, M. (2009). Tubulin tyrosination navigates the kinesin-1 motor domain to axons. *Nat. Neurosci.* **12**, 559-567.

Kovacs, J. J., Cohen, T. J. and Yao, T. P. (2005). Chaperoning steroid hormone signaling via reversible acetylation. *Nucl. Recept. Signal.* **3**, e004.

Kwon, S., Zhang, Y. and Matthias, P. (2007). The deacetylase HDAC6 is a novel critical component of stress granules involved in the stress response. *Genes Dev.* **21**, 3381-3394.

Lansbergen, G. and Akhmanova, A. (2006). Microtubule plus end: a hub of cellular activities. *Traffic* **7**, 499-507.

LeDizet, M. and Piperno, G. (1987). Identification of an acetylation site of Chlamydomonas alpha-tubulin. *Proc. Natl. Acad. Sci. USA* **84**, 5720-5724.

L'Hernault, S. W. and Rosenbaum, J. L. (1985). Chlamydomonas alpha-tubulin is posttranslationally modified by acetylation on the epsilon-amino group of a lysine. *Biochemistry* **24**, 473-478.

Liao, G. and Gundersen, G. G. (1998). Kinesin is a candidate for cross-bridging microtubules and intermediate filaments. Selective binding of kinesin to detyrosinated tubulin and vimentin. *J. Biol. Chem.* **273**, 9797-9803.

Ligon, L. A., Shelly, S. S., Tokito, M. and Holzbaur, E. L. (2003). The microtubule plus-end proteins EB1 and dynactin have differential effects on microtubule polymerization. *Mol. Biol. Cell* **14**, 1405-1417.

Loktev, A. V., Zhang, Q., Beck, J. S., Searby, C. C., Scheetz, T. E., Bazan, J. F., Slusarski, D. C., Sheffield, V. C., Jackson, P. K. and Nachury, M. V. (2008). A BBSome subunit links ciliogenesis, microtubule stability, and acetylation. *Dev. Cell* **15**, 854-865.

Mahadevan, L. and Mitchison, T. J. (2005). Cell biology: powerful curves. *Nature* **435**, 895-897.

Margolis, R. L. and Wilson, L. (1977). Addition of colchicine-tubulin complex to microtubule ends: the mechanism of substoichiometric colchicine poisoning. *Proc. Natl. Acad. Sci. USA* **74**, 3466-3470.

Maruta, H., Greer, K. and Rosenbaum, J. L. (1986). The acetylation of alpha-tubulin and its relationship to the assembly and disassembly of microtubules. *J. Cell Biol.* **103**, 571-579.

Matsuyama, A., Shimazu, T., Sumida, Y., Saito, A., Yoshimatsu, Y., Seigneurin-Berny, D., Osada, H., Komatsu, Y., Nishino, N., Khochbin, S. et al. (2002). In vivo destabilization of dynamic microtubules by HDAC6-mediated deacetylation. *EMBO J.* **21**, 6820-6831.

Matthias, P., Yoshida, M. and Khochbin, S. (2008). HDAC6 a new cellular stress surveillance factor. *Cell Cycle* **7**, 7-10.

Mimori-Kiyosue, Y. and Tsukita, S. (2003). "Search-and-capture" of microtubules through plus-end-binding proteins (+TIPs). *J. Biochem. (Tokyo)* **134**, 321-326.

Mimori-Kiyosue, Y., Shiina, N. and Tsukita, S. (2000). The dynamic behavior of the APC-binding protein EB1 on the distal ends of microtubules. *Curr. Biol.* **10**, 865-868.

Mishima, M., Maesaki, R., Kasa, M., Watanabe, T., Fukata, M., Kaibuchi, K. and Hakoshima, T. (2007). Structural basis for tubulin recognition by cytoplasmic linker protein 170 and its autoinhibition. *Proc. Natl. Acad. Sci. USA* **104**, 10346-10351.

Morrison, E. E. (2007). Action and interactions at microtubule ends. *Cell Mol. Life Sci.* **64**, 307-317.

Nahhas, F., Dryden, S. C., Abrams, J. and Tainsky, M. A. (2007). Mutations in SIRT2 deacetylase which regulate enzymatic activity but not its interaction with HDAC6 and tubulin. *Mol. Cell Biochem.* **303**, 221-230.

Nogales, E. (1999). A structural view of microtubule dynamics. *Cell Mol. Life Sci.* **56**, 133-142.

Nogales, E. and Wang, H. W. (2006). Structural mechanisms underlying nucleotide-dependent self-assembly of tubulin and its relatives. *Curr. Opin. Struct. Biol.* **16**, 221-229.

Nogales, E., Whittaker, M., Milligan, R. A. and Downing, K. H. (1999). High-resolution model of the microtubule. *Cell* **96**, 79-88.

North, B. J., Marshall, B. L., Borra, M. T., Denu, J. M. and Verdin, E. (2003). The human Sir2 ortholog, SIRT2, is an NAD+-dependent tubulin deacetylase. *Mol. Cell* **11**, 437-444.

Palazzo, A., Ackerman, B. and Gundersen, G. G. (2003). Cell biology: Tubulin acetylation and cell motility. *Nature* **421**, 230.

Park, S. J., Suetsugu, S. and Takenawa, T. (2005). Interaction of HSP90 to N-WASP leads to activation and protection from proteasome-dependent degradation. *EMBO J.* **24**, 1557-1570.

Perez, M., Santa-Maria, I., Gomez de Barreda, E., Zhu, X., Cuadros, R., Cabrero, J. R., Sanchez-Madrid, F., Dawson, H. N., Vitek, M. P., Perry, G. et al. (2009). Tau-an inhibitor of deacetylase HDAC6 function. *J. Neurochem.* **109**, 1756-1766.

Peris, L., Thery, M., Faure, J., Saoudi, Y., Lafanechere, L., Chilton, J. K., Gordon-Weeks, P., Galjart, N., Bornens, M., Wordeman, L. et al. (2006). Tubulin tyrosination is a major factor affecting the recruitment of CAP-Gly proteins at microtubule plus ends. *J. Cell Biol.* **174**, 839-849.

Peris, L., Wagenbach, M., Lafanechere, L., Brocard, J., Moore, A. T., Kozielski, F., Job, D., Wordeman, L. and Andrieux, A. (2009). Motor-dependent microtubule disassembly driven by tubulin tyrosination. *J. Cell Biol.* **185**, 1159-1166.

Piperno, G., LeDizet, M. and Chang, X. J. (1987). Microtubules containing acetylated alpha-tubulin in mammalian cells in culture. *J. Cell Biol.* **104**, 289-302.

Reed, N. A., Cai, D., Blasius, T. L., Jih, G. T., Meyhofer, E., Gaertig, J. and Verhey, K. J. (2006). Microtubule acetylation promotes kinesin-1 binding and transport. *Curr. Biol.* **16**, 2166-2172.

Sammak, P. J. and Borisy, G. G. (1988). Direct observation of microtubule dynamics in living cells. *Nature* **332**, 724-726.

Scott, G. K., Marx, C., Berger, C. E., Saunders, L. R., Verdin, E., Schafer, S., Jung, M. and Benz, C. C. (2008). Destabilization of ERBB2 transcripts by targeting 3′ untranslated region messenger RNA associated HuR and histone deacetylase-6. *Mol. Cancer Res.* **6**, 1250-1258.

Serrador, J. M., Cabrero, J. R., Sancho, D., Mittelbrunn, M., Urzainqui, A. and Sanchez-Madrid, F. (2004). HDAC6 deacetylase activity links the tubulin cytoskeleton with immune synapse organization. *Immunity* **20**, 417-428.

Shelden, E. and Wadsworth, P. (1990). Interzonal microtubules are dynamic during spindle elongation. *J. Cell Sci.* **97**, 273-281.

Thompson, W. C. (1982). The cyclic tyrosination/detyrosination of alpha tubulin. *Methods Cell Biol.* **24**, 235-255.

Tran, A. D., Marmo, T. P., Salam, A. A., Che, S., Finkelstein, E., Kabarriti, R., Xenias, H. S., Mazitschek, R., Hubbert, C., Kawaguchi, Y. et al. (2007). HDAC6 deacetylation of tubulin modulates dynamics of cellular adhesions. *J. Cell Sci.* **120**, 1469-1479.

Valenzuela-Fernandez, A., Cabrero, J. R., Serrador, J. M. and Sanchez-Madrid, F. (2008). HDAC6: a key regulator of cytoskeleton, cell migration and cell-cell interactions. *Trends Cell Biol.* **18**, 291-297.

Valiron, O., Caudron, N. and Job, D. (2001). Microtubule dynamics. *Cell Mol. Life Sci.* **58**, 2069-2084.

Verhey, K. J. and Gaertig, J. (2007). The tubulin code. *Cell Cycle* **6**, 2152-2160.

Webster, D. R. and Borisy, G. G. (1989). Microtubules are acetylated in domains that turn over slowly. *J. Cell Sci.* **92**, 57-65.

Westermann, S. and Weber, K. (2003). Post-translational modifications regulate microtubule function. *Nat. Rev. Mol. Cell. Biol.* **4**, 938-947.

Wittmann, T., Bokoch, G. M. and Waterman-Storer, C. M. (2004). Regulation of microtubule destabilizing activity of Op18/stathmin downstream of Rac1. *J. Biol. Chem.* **279**, 6196-6203.

Zhang, X., Yuan, Z., Zhang, Y., Yong, S., Salas-Burgos, A., Koomen, J., Olashaw, N., Parsons, J. T., Yang, X. J., Dent, S. R. et al. (2007). HDAC6 Modulates cell motility by altering the acetylation level of cortactin. *Mol. Cell* **27**, 197-213.

Zhang, Y., Li, N., Caron, C., Matthias, G., Hess, D., Khochbin, S. and Matthias, P. (2003). HDAC-6 interacts with and deacetylates tubulin and microtubules in vivo. *EMBO J.* **22**, 1168-1179.

Zhang, Y., Gilquin, B., Khochbin, S. and Matthias, P. (2006). Two catalytic domains are required for protein deacetylation. *J. Biol. Chem.* **281**, 2401-2404.

Zhang, Y., Kwon, S., Yamaguchi, T., Cubizolles, F., Rousseaux, S., Kneissel, M., Cao, C., Li, N., Cheng, H. L., Chua, K. et al. (2008). Mice lacking histone deacetylase 6 have hyperacetylated tubulin but are viable and develop normally. *Mol. Cell. Biol.* **28**, 1688-1701.

Zhou, J., Vos, C. C., Gjyrezi, A., Yoshida, M., Khuri, F. R., Tamanoi, F. and Giannakakou, P. (2009). The protein farnesyltransferase regulates HDAC6 activity in a microtubule-dependent manner. *J. Biol. Chem.* **284**, 9648-9655.

Zigmond, S. H., Evangelista, M., Boone, C., Yang, C., Dar, A. C., Sicheri, F., Forkey, J. and Pring, M. (2003). Formin leaky cap allows elongation in the presence of tight capping proteins. *Curr. Biol.* **13**, 1820-1823.

Journal of Cell Science